DOI: 10.1002/ejic.200800548

Manganese(II) Trimeric Systems Derived from Pyridyldioximato Ligands: Synthesis, Crystal Structure, and Magnetic Characterization

Albert Escuer,*[a] Beatriz Cordero,[a] Xavier Solans,[b][†] Mercé Font-Bardia,[b] and Teresa Calvet[b]

Keywords: Manganese / Oximato ligands / Magnetic properties / Carboxylato bridges / Structural determination

Three new manganese compounds have been obtained by reaction of the 2,6-diacetylpyridine dioxime (dapdoH_2) ligand with several Mn^{II} salts. By using a variety of manganese(II) carboxylates, three Mn^{II} derivatives with general formula $[Mn_3(RCOO)_6(dapdoH_2)_2]$, where $RCOO^-$ = formate (**1**), acetate (**2**), and benzoate (**3**), were obtained. Structural analysis reveals chains of trinuclear units for **1** and isolated trinuclear molecules for **2**. Compound **1** provides an example of a new topology for the $[Mn_3(RCOO)_6(L)_2]$ general formula. Magnetic susceptibility studies reveal topological ferrimagnetism for **1** and conventional antiferromagnetic response for **2** and **3**, with coupling constants of –3.1, –3.2, and –1.4 cm^{-1} inside the trimeric units of **1**, **2**, and **3**, respectively.

Introduction

Manganese chemistry is a field of coordination chemistry that has received continuous attention over the past decades. Its ability to provide stable compounds in several oxidation states, the redox transitions that easily take place between them, together with the relevant magnetic properties of the Mn^{III} oxidation state are some of the reasons that have motivated this permanent research either in the field of bioinorganic modeling or in the search for high-spin clusters with single-molecule magnet (SMM) properties. One of the crucial components of this kind of work is the design of reactions with new ligands, which are able to improve the routes of synthesis or the properties of the resulting systems. R-2-pyridyl ketone oximes, in which R = H, Me, Ph, py, or *t*Bu, have been widely employed with excellent results by several authors with a variety of transition-metal ions in cluster chemistry.[1] Around 40 manganese/R-2-pyridyl ketoxime derivatives, with nuclearities ranging from mononuclear to Mn_8,[2] Mn_9,[3] Mn_{10},[4] or Mn_{12},[5] have been reported in the last few years. In contrast, the reactivity of 2,6-pyridyldioximato ligands and their ability to generate high-nuclearity clusters remains practically unexplored, in spite of their good coordination possibilities. 2,6-Diacetylpyridine dioxime (dapdoH_2) acts as a tridentate N-donor in its neutral form, but the two oximato arms in the dapdoH^- or dapdo^{2-} deprotonated forms are potentially useful to generate high-nuclearity systems with new topologies.

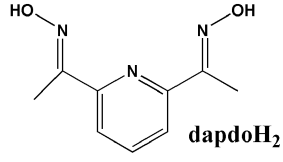

dapdoH_2

To date, only one Cu^{II} dinuclear and one $Fe^{II,III}$ trinuclear system have been reported in addition to some mononuclear complexes.[6] However, very recently one Cr_2Cu_2 and some relevant hexa- and octanuclear $Mn^{II,III}$ derivatives have been obtained and studied.[7]

Following our previous work in this field, we have extended our research to the exploration of the reactivity of dapdoH_2 with a variety of carboxylates, obtaining the trinuclear Mn^{II} derivatives $[Mn_3(RCOO)_6(dapdoH_2)_2]$, in which R = formate (**1**), acetate (**2**), and benzoate (**3**). The synthesis, structure, and magnetic properties of the new compounds are described.

Results and Discussion

Description of the Structures

$[Mn_3(HCOO)_6(dapdoH_2)_2]_n$ (**1**) can be described as chains of centrosymmetric trinuclear Mn^{2+} subunits linked by double *anti-anti* formato bridges (Figure 1). The trinuclear subunits consist of a linear arrangement of three manganese atoms bridged by four carboxylato bridges and two

[a] Departament de Química Inorgànica and Institut de Nanociència i Nanotecnologia de la Universitat de Barcelona (IN2UB), Martí Franqués 1-11, 08028 Barcelona, Spain
Fax: +34-934907725
E-mail: albert.escuer@qi.ub.es
[b] Departament de Mineralogia I Cristallografia, Universitat de Barcelona,
Martí Franqués s/n, 08028 Barcelona, Spain
[†] Deceased

dapdoH_2 ligands acting as tridentate *N*,*N*′,*N*′′-donors on the terminal Mn(2) ions. The coordination polyhedron around Mn(2) is a very distorted octahedron because of the N(1)–Mn(2)–N(2) and N(2)–Mn(2)–N(3) bond angles with values of 70.03(8)° and 68.40(8)°, respectively. The remaining coordination sites are occupied by three oxygen atoms from three different carboxylates, giving a MnN_3O_3 environment.

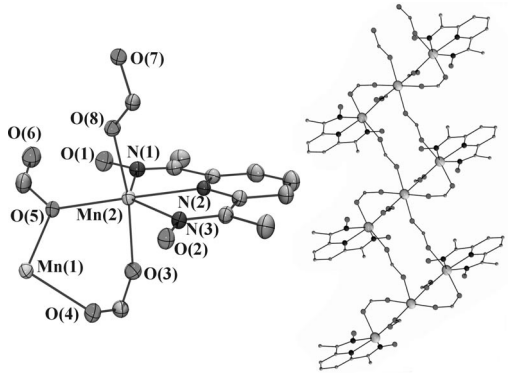

Figure 1. Left: labeled ORTEP plot (ellipsoid at 20% probability) for the asymmetric unit of $[Mn_3(HCOO)_6(dapdoH_2)_2]_n$ (**1**). Right: 1D arrangement of trinuclear subunits for **1**.

The central Mn(1) atom shows a quite regular octahedral MnO_6 environment with four bridging formato ligands, which link Mn(1) with both Mn(2) atoms by means of double carboxylato bridges, and two *anti-anti* formato bridges which link it with Mn(2′) from neighboring trinuclear units. This compound simultaneously exhibits three coordination modes for the formato ligand: *syn-syn* Mn(1)–O(4)–C(10)–O(3)–Mn(2) with a torsion angle Mn(1)–O(4)···O(3)–Mn(2) of 43.9°, monatomic μ_2-O,O bridges Mn(1)–O(5)–Mn(2) with a bond angle of 112.83°, and *anti-anti* Mn(2)–O(7)–C(12)–O(8)–Mn(1′) bridges with a torsion angle Mn(2)–O(8)···O(7)–Mn(1′) of 5.2°. Mn(1)···Mn(2) distances inside the trimeric units are 3.659 Å, and intertrimer Mn(2)···Mn(1′) distances across the *anti-anti* formato bridges are 6.108 Å.

The hydrogen atoms of the protonated oximato groups provide intramolecular hydrogen bonds: O(1)–H(1)···O(6) involves the noncoordinated O(6) atom from one of the formato ligands, whereas O(2)–H(2)···O(7) relates the second oximato with the *anti-anti* formato ligand. No short interchain hydrogen bonds were found.

$[Mn_3(MeCOO)_6(dapdoH_2)]$ (**2**) can be described as a centrosymmetric linear trinuclear system in which the two dapdoH_2 ligands act as tridentate *N*,*N*′,*N*′′-donors to the terminal Mn(2) atoms, whereas the six acetate ligands bridge them to the central Mn(1) atom (Figure 2).

The N(1)–Mn(2)–N(2) and N(2)–Mn(2)–N(3) bond angles show values of 66.73(7)° and 69.04(8)°, allowing heptacoordination around Mn(2). The remaining coordination sites are occupied by one bidentate acetate ligand with an O(5)–Mn(2)–O(6) bond angle of 56.10(7)° and O(1) and O(4) atoms from two different acetate groups, giving a MnN_3O_4 environment. The polyhedron around Mn(2) can

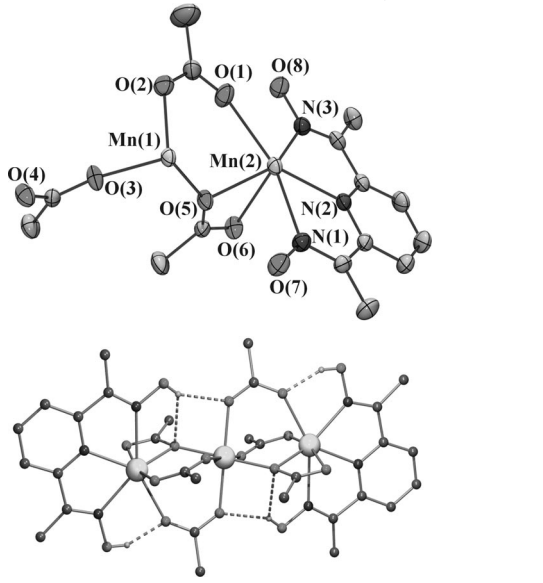

Figure 2. Top: labeled ORTEP plot (ellipsoid at 20% probability) for the asymmetric unit of $[Mn_3(MeCOO)_6(dapdoH_2)_2]$ (**2**). Bottom: a view of trinuclear compound **2**. Dashed lines show the intramolecular hydrogen bonds.

be described as a distorted pentagonal bipyramid with O(4′) and O(6) in the axial positions.

In contrast, Mn(1) exhibits a quite regular octahedral MnO_6 environment with the six coordination sites occupied by six oxygen atoms from the six acetato bridging ligands. Two of the acetates act as *syn-syn* bridges between each Mn(2) and Mn(1), whereas the third acetate exhibits the μ_2-*O*,*O*,*O*′ coordination mode with a Mn(1)–O(5)–Mn(2) bond angle of 111.70(8)°. Mn(1)···Mn(2) intertrimer distances are 3.603 Å.

The hydrogen atoms of the protonated oximato groups give a set of intramolecular hydrogen bonds that involve two carboxylates: one of the oximato groups interacts by means of O(7)–H(7o)···O(5) and O(7)–H(7o)···O(2) hydrogen bonds, and the second oximate group provides the O(8)–H(8o)···O(1) interaction. No short intermolecular hydrogen bonds have been observed.

There are a limited number of linear Mn^{II}_3 compounds with six bridging carboxylates that can be classified into two general types: in one of them, with general formula $[Mn_3(RCOO)_6(L)_6]$ (L = monodentate donor), all the carboxylato ligands are coordinated in the *syn-syn* mode, giving a triple bridge between the central and external manganese atoms (Scheme 1a).[8] The second type, with general formula $[Mn_3(RCOO)_6(LL)_2]$ (LL = bidentate ligand), is quite similar with the central manganese atom coordinated to six carboxylato ligands, whereas the coordination sphere of the terminal Mn^{II} atoms has two coordination sites occupied by the bidentate LL ligand and reaches hexacoordination by means of two s*yn-syn* carboxylato bridges and one μ_2-carboxylato-*O*,*O*,*O*′ ligand (Scheme 1b).[2b,9,10] In our case, the use of the tridentate planar dapdoH_2 ligand yields the second type of carboxylato arrangement for **2** (Scheme 1b). However, in this case the terminal manganese

atoms are heptacoordinated with a coordination polyhedron close to a pentagonal bipyramid, giving the first example of the general formula $[Mn_3(RCOO)_6(LLL)_2]$ (LLL = tridentate ligand). Compound **1** has the same general formula but exhibits a new topology, in which two of the carboxylato ligands act as *anti-anti* bridges between the trinuclear units, giving a 1D $[Mn_3]_n$ system.

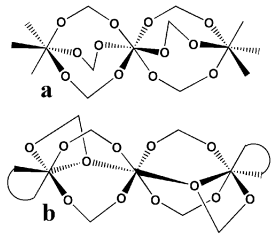

Scheme 1. Typical $\{Mn_3(RCOO)_6\}$ cores.

Magnetic Measurements

Solid-state susceptibility measurements, performed on powdered samples in the 300–2 K range indicate an overall intramolecular antiferromagnetic behavior for **2** and **3**. The $\chi_M T$ values at room temperature for compounds **2** and **3** are 13.04 and 13.40 $cm^3 K mol^{-1}$, decreasing continuously to 4.31 and 4.54 $cm^3 K mol^{-1}$, respectively, on cooling down to 2 K (Figure 3). From analytical data, the $\chi_M T$ values and the overall shape of the susceptibility plots, we assume that benzoato derivative **3** has a manganese arrangement similar to that of **2**. Room-temperature values for both compounds are slightly lower than that expected for three isolated Mn^{II} atoms (13.125 $cm^3 K mol^{-1}$ assuming $g = 2.00$), whereas the low-temperature value agrees with one $S = 5/2$ ground state. Fitting of the experimental data was performed by using the conventional analytical equation derived from the Hamiltonian.

$$H = -J_1(S_1S_2 + S_2S_3) - J_2(S_1S_3)$$

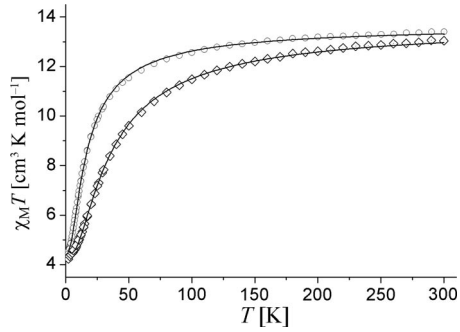

Figure 3. Plot of $\chi_M T$ vs. T for compounds **2** (diamonds) and **3** (circles). The solid lines represent the best theoretical fit (see text).

Best fit parameters were $J_1 = -3.2(1)$ cm^{-1} for **2** and $-1.4(1)$ cm^{-1} for **3**, negligible J_2 values less than -0.1 cm^{-1}, and $g = 2.050(1)$ and $2.041(1)$ for **2** and **3**, respectively.

Magnetization experiments performed at 2 K show that the plots with a Brillouin-like shape, which are similar to a curve for five electrons, confirm the S = 5/2 ground state for **2** and **3** (Figure 4). The high field deviation of the plot for **3** is consistent with the lower J value which allows mixing with the closer excited $S = 7/2$ level under high external fields.

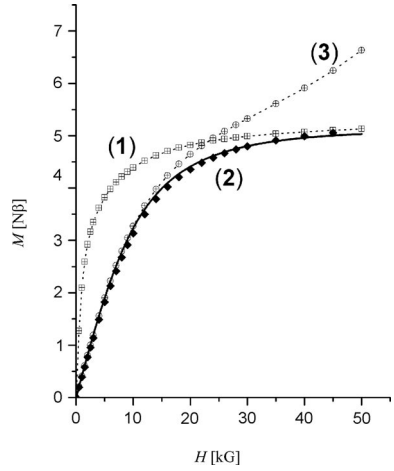

Figure 4. Molar magnetization vs. external field for compounds **1**–**3**. Dotted lines are eye guides. The solid line corresponds to the Brillouin plot for an isolated $S = 5/2$ spin and $g = 2.05$.

J_1 values found for compounds **2** and **3** are in full agreement with previously reported $[Mn_3(RCOO)_6(LL)_2]$ systems with the same topology (Scheme 1b), for which J values lying in the range -1.2/-5.6 cm^{-1} have been found. As can be seen in Table 1, any correlation can be deduced from the structural data involving the μ_2-*O*,*O*,*O*′ carboxylato ligand and the J coupling constant.

Table 1. Selected structural and magnetic data for $[Mn_3(RCOO)_6(LL)_2]$ trinuclear systems with topology as in Scheme 1b. O and O′ refer to the two oxygen atoms of the bridging μ_2-*O*,*O*,*O*′ carboxylato ligands.

Compound (LL[a])	Mn–O–Mn	Mn–O′ [Å]	J_1	Ref.
$[Mn_3(BzO)_6(2\text{-bzpy})_2]$	106.31°	2.250	–2.7	[2b]
$[Mn_3(AcO)_6(bpy)_2]$	112.12°	2.606	–4.4	[10a]
$[Mn_3(AcO)_6(AcO)_2]$	113.05°	2.203	–5.6	[10b]
$[Mn_3(ClCH_2COO)_6(bpy)_2]$	112.12°	2.611	–3.8	[10d]
$[Mn_3(AcO)_6(mim)_2]$	110.60°	2.341	–1.2	[10e]
$[Mn_3(AcO)_6(dapdoH_2)_2]$	111.70°	2.402	–3.2	this work

[a] 2-bzpy = phenyl-2-pyridyl ketone; bpy = 2,2′-bipyridyl; mim = 1-methylimidazol-2-ylmethanone.

Compound **1** exhibits a similar high-temperature response, but in contrast to the above measurements, the low-temperature behavior is clearly different. The $\chi_M T$ value at room temperature for compound **1** is 13.10 $cm^3 K mol^{-1}$, decreasing continuously down to 6.30 $cm^3 K mol^{-1}$ on cooling to 12 K. Below this well-defined minimum, the $\chi_M T$ value quickly increases up to a value of 31.45 $cm^3 K mol^{-1}$ at 2 K (Figure 5). Magnetization measurements performed at 2 K show a magnetization plot that is similar to a curve for five electrons of a trinuclear unit with a non-Brillouin shape, which is in agreement with the ferromagnetic response of this compound at low temperature (Figure 4). The structural and magnetic data indicates a high-temperature behavior similar to that of the trinuclear compounds **2** and **3**, whereas at low temperatures, the intertrimer *anti-anti*

formato bridges seem to induce weak ferromagnetic interactions. The absence of decay in $\chi_M T$ even at 2 K indicates that the chains are very well isolated and interchain interactions become negligible.

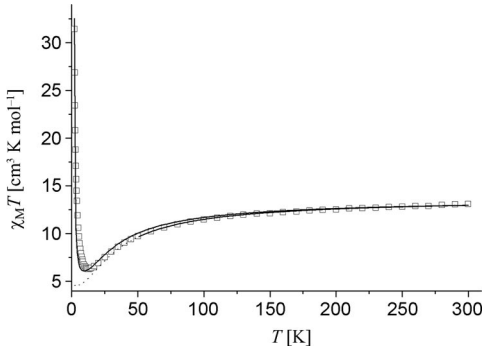

Figure 5. Plot of $\chi_M T$ vs. T for compound **1**. The solid lines represent the best theoretical fits between room temperature and 2 K (taking into account intertrimer interactions) and as isolated trinuclear units between room temperature and 50 K, the dotted line being the calculated values below 50 K for the latest data.

Because of the shape of the $\chi_M T$ plot, the fit of the experimental data was performed by assuming that the interactions inside the trinuclear unit are much greater than the ones induced by the *anti-anti* formato bridges, which are only operative at temperatures below the minimum of $\chi_M T$. Fitting of the $\chi_M T$ plot as a trinuclear unit and discarding the low-temperature data (300–50 K range) gives as a best fit $J_1 = -3.15(4)$ cm^{-1}, a negligible J_2 value lower than –0.1 cm^{-1}, and $g = 2.048(2)$.

A second fit, as a rough approach to the low-temperature interactions, was performed by assuming the interaction along the chain to be a zJ' perturbation ($z = 2$ neighbors). Fitting the experimental data under these conditions gives as the best result the reasonable values $J_1 = -3.0(2)$ cm^{-1}, $g = 2.04(1)$, and $zJ' = +1.7(1)$. These values are consistent for J_1 and g. However, the intertrimer interaction, despite its positive sign that seems in good agreement with the increase in $\chi_M T$ below 12 K, should be carefully analyzed.

Single carboxylato bridges give typically weak interactions, mainly in the *syn-anti* or *anti-anti* coordination modes. To date, some scarce *anti-anti* formato bridges have been reported, and in all cases, very weak or negligible antiferromagnetic coupling has been found.[11] In our case, the low-temperature ferromagnetic interactions can be analyzed by means of the coupling scheme (Scheme 2). If we assume that intertrimer interactions promoted by the formato bridges are ferromagnetic in nature and weaker than the J_1 intratrimer interactions (Scheme 2A), then the total spin of the system tends to zero because all the spins become antiparallel, whereas if the interactions promoted by the formato bridges are antiferromagnetic, although the spins related to the *anti-anti* formato bridges cancel one another, the spin of the nonbridged manganese atoms remains parallel. Both susceptibility and magnetization experiments indicate a $S = 5/2$ ground state; therefore, coupling Scheme 2B should be assumed as correct.

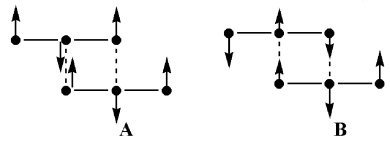

Scheme 2. Ferromagnetic (A) and antiferromagnetic (B) *anti-anti* formato interaction scheme for the chain of trinuclear subunits in compound **1**.

This implies that the interaction mediated by the formato bridges is, as usual, weakly antiferromagnetic, and the increase in $\chi_M T$ below 12 K is due to a topologic ferrimagnetism. The positive sign of zJ' is only a mathematical artifact and is not directly related to the formato bridge.

Conclusions

We have reported the reactivity of the dapdoH_2 ligand with Mn^{II} carboxylates and the general trend of the stabilization of the divalent oxidation state even in moderately basic medium. The reported compounds **1**–**3** have the same general formula [Mn(RCOO)$_6$(dapdoH_2)$_2$], but for the first time heptacoordination on the terminal manganese atoms has been found for the case of the acetato derivative, whereas a new structural topology has been found for the chain of trimers derived from the formato ligand.

Experimental Section

General Remarks: Magnetic susceptibility measurements were carried out on polycrystalline samples with a Quantum Design susceptometer working in the range 2–300 K under magnetic fields of 0.3 T and remeasured under a field of 0.03 T in the 20–2 K range. Diamagnetic corrections were estimated from Pascal tables. Infrared spectra (4000–400 cm^{-1}) were recorded from KBr pellets.

Synthetic Aspects: Reactions of dapdoH_2 in methanol with several manganese carboxylates were carried out under neutral and mildly basic conditions by addition of Et_3N. In contrast with other pyridylmonoximes, the solutions were not oxidized under ambient conditions, yielding in all cases yellow derivatives of Mn^{2+}. Even when manganese(III) acetate was used as a starting reagent and its mixture with the ligand was layered with ether, the resulting dark solutions yielded yellow crystals of **2** in a few days, after progressive discoloration of the solution. In very strong basic media, the manganese/carboxylate solutions changed to dark brown, but well-defined compounds have not been isolated. Consequently, the following experimental procedure for the synthesis of compounds **1**–**3** is described without addition of basic medium.

[Mn$_3$(HCOO)$_6$(dapdoH$_2$)$_2$] (1): The complete synthesis was carried out under N_2 because of the presence of small quantities of brown impurities in the aerobic synthesis. Mn(HCOO)$_2$·xH$_2$O (163 mg, 1 mmol) and L (193 mg, 1 mmol) were dissolved in MeOH (20 mL). Upon layering the resulting yellow solution with diethyl ether, well-formed yellow crystals of compound **1** were obtained in two days in a 20% yield. $C_{24}H_{28}Mn_3N_6O_{16}$ (821.34): calcd. C 35.10, H 3.44, N 10.23; found C 35.0, H 3.4, N 10.4. IR: $\tilde{\nu}$ = 2819 (m), 1591 (s), 1354 (s), 1046 (m), 768 (m) cm^{-1}.

[Mn$_3$(MeCOO)$_6$(dapdoH$_2$)$_2$] (2): Mn(AcO)$_2$·4H$_2$O (245 mg, 1 mmol) dissolved in MeOH (10 mL) was mixed with a solution of

L (193 mg, 1 mmol) in methanol (10 mL). Upon layering the resulting yellowish solution with diethyl ether, large yellow prismatic crystals of compound **2** were obtained in three days in 40% yield. $C_{30}H_{40}Mn_3N_6O_{16}$ (905.50): calcd. C 39.79, H 4.45, N 9.28; found C 39.6, H 4.3, N 9.4. IR: $\tilde{\nu}$ = 3422 (s), 1588 (s), 1419 (s), 1020 (m), 811 (m), 690 (m) cm^{-1}.

$[Mn_3(BzCOO)_6(dapdoH_2)_2]$ (3): $Mn(BzO)_2{\cdot}2H_2O$ (333 mg, 1 mmol) dissolved in MeOH (5 mL) was mixed with a solution of L (193 mg, 1 mmol) in methanol (10 mL). Upon layering the resulting yellowish solution with diethyl ether, yellow microcrystalline compound **3** was obtained in 30% yield. $C_{60}H_{52}Mn_3N_6O_{16}$ (1277.90): calcd. C 56.39, H 4.10, N 6.58; found C 56.0, H 4.0, N 6.5. IR: $\tilde{\nu}$ = 3397 (s), 1603 (s), 1404 (s), 1028 (m), 714 (m) cm^{-1}.

Table 2. Parameters for data collection and structure refinement for compounds **1** and **2**.

Compound	**1**	**2**
Formula	$C_{24}H_{28}Mn_3N_6O_{16}$	$C_{30}H_{40}Mn_3N_6O_{16}$
M	821.34	905.50
Space group	$P2_1/c$	$P\bar{1}$
Crystal system	monoclinic	triclinic
a [Å]	7.775(5)	8.058(3)
b [Å]	20.688(10)	9.922(9)
c [Å]	10.602(4)	13.491(6)
α [°]	90	106.60(5)
β [°]	108.28(3)	95.61(3)
γ [°]	90	106.13(5)
U [Å^3]	1619.3(14)	974.4(11)
Z	2	1
T [K]	293(2)	293(2)
$D_{calcd.}$ [g cm^{-3}]	1.685	1.543
$F(000)$	834	465
μ(Mo-K_α) [mm^{-1}]	1.234	1.033
Measured reflections	3746	5651
Unique reflections	3746	5650
R_{int}	0.048	0.036
$[I > 2\sigma(I)]$	3746	4567
$\theta_{min}/\theta_{max}$ [°]	2.76 to 31.02	2.3 to 30.0
$R(F^2)$	0.0412	0.0363
$wR(F^2)$	0.1001	0.1019
No. variables	233	283
$\Delta\rho_{max}$; $\Delta\rho_{min}$ [e Å^{-3}]	–0.434/0.544	–0.35/0.61

Table 3. Selected interatomic distances for compounds **1** and **2**.

Compound **1**	[Å]	Compound **2**	[Å]
Mn(1)–O(4)	2.161(2)	Mn(1)–O(2)	2.150(3)
Mn(1)–O(5)	2.202(2)	Mn(1)–O(3)	2.199(3)
Mn(1)–O(7b)	2.176(2)	Mn(1)–O(5)	2.161(2)
Mn(2)–O(3)	2.105(2)	Mn(2)–O(1)	2.375(3)
Mn(2)–O(5)	2.190(2)	Mn(2)–O(5)	2.193(2)
Mn(2)–O(8)	2.119(2)	Mn(2)–O(6)	2.402(3)
Mn(2)–N(1)	2.271(2)	Mn(2)–N(1)	2.474(3)
Mn(2)–N(2)	2.247(2)	Mn(2)–N(2)	2.298(3)
Mn(2)–N(3)	2.387(2)	Mn(2)–N(3)	2.288(3)
		Mn(2)–O(4a)	2.090(2)
O(1)–N(1)	1.383(3)	O(7)–N(1)	1.390(3)
N(1)–C(2)	1.272(4)	N(1)–C(8)	1.283(3)
O(2)–N(3)	1.375(3)	O(8)–N(3)	1.390(3)
N(3)–C(8)	1.279(3)	N(3)–C(14)	1.282(3)
O(3)–C(10)	1.244(4)	O(1)–C(1)	1.241(3)
O(4)–C(10)	1.230(3)	O(2)–C(1)	1.248(3)
O(5)–C(11)	1.259(4)	O(3)–C(3)	1.248(3)
O(6)–C(11)	1.225(4)	O(4)–C(3)	1.256(2)
O(7)–C(12)	1.260(3)	O(5)–C(5)	1.269(2)
O(8)–C(12)	1.221(3)	O(6)–C(5)	1.237(2)

Crystallography: Prismatic crystals were selected and mounted on a MAR345 diffractometer with an image plate detector for **1** and an Enraf–Nonius CAD4 four-circle diffractometer for **2**. The structure was solved by direct methods with the SHELXS computer program[12] and refined by full-matrix least-squares methods with SHELX97.[13] The function minimized was $\Sigma w||F_o|^2 - |F_c|^2|^2$, where $w = [\sigma 2(I) + (0.0507P)^2 + 0.2307P]^{-1}$ for (**1**), $w = [\sigma 2(I) + (0.0554P)^2 + 0.1782P]^{-1}$ for (**2**), and $P = (|F_o|^2 + 2|F_c|^2)/3$. f, f', and f'' were taken from the International Tables of X-ray Crystallography.[14] For compound **1**, all H atoms were computed and refined, using a riding model, with an isotropic temperature factor equal to 1.2-times the equivalent temperature factor of the atoms which are linked; for compound **2**, five H atoms were located from a difference synthesis and refined with an overall isotropic temperature factor, and 15 H atoms were computed and refined, using a riding model, with an isotropic temperature factor equal to 1.2-times the equivalent temperature factor of the atoms which are linked. Details of the data collection and refinement and bond parameters are summarized in Tables 2, 3, and 4.

CCDC-688263 (**1**) and -688264 (**2**) contain the supplementary crystallographic data for this paper. These data can be obtained free of charge from the Cambridge Crystallographic Data Centre via www.ccdc.cam.ac.uk/datarequest/cif.

Table 4. Selected bond angles for compounds **1** and **2**.

Compound **1**	[°]	Compound **2**	[°]
O(5)–Mn(1)–O(4)	90.07(7)	O(2)–Mn(1)–O(3)	87.51(8)
O(5)–Mn(1)–O(4a)	89.93(7)	O(2)–Mn(1)–O(5)	94.87(8)
O(5)–Mn(1)–O(5a)	180	O(2)–Mn(1)–O(2a)	180
O(5)–Mn(1)–O(7b)	90. 93(7)	O(2)–Mn(1)–O(3a)	92.49(8)
O(5)–Mn(1)–O(7c)	89.07(7)	O(2)–Mn(1)–O(5a)	85.13(8)
O(4)–Mn(1)–O(4a)	180	O(3)–Mn(1)–O(5)	91.72(7)
O(4)–Mn(1)–O(7b)	90.88(7)	O(3)–Mn(1)–O(3a)	180
O(4)–Mn(1)–O(7c)	89.12(7)	O(3)–Mn(1)–O(5a)	88.29(7)
O(7b)–Mn(1)–O(7c)	180	O(5)–Mn(1)–O(5a)	180
O(3)–Mn(2)–O(5)	86.26(8)	O(1)–Mn(2)–O(5)	80.69(7)
O(3)–Mn(2)–O(8)	165.54(8)	O(1)–Mn(2)–O(6)	99.58(7)
O(3)–Mn(2)–N(1)	93.62(8)	O(1)–Mn(2)–N(1)	151.32(8)
O(3)–Mn(2)–N(2)	89.60(8)	O(1)–Mn(2)–N(2)	141.43(8)
O(3)–Mn(2)–N(3)	88.41(9)	O(1)–Mn(2)–N(3)	72.67(8)
O(5)–Mn(2)–O(8)	84.35(8)	O(1)–Mn(2)–O(4a)	86.12(8)
O(5)–Mn(2)–N(1)	100.70(8)	O(5)–Mn(2)–O(6)	56.10(7)
N(1)–Mn(2)–N(2)	70.03(8)	O(5)–Mn(2)–N(1)	77.95(7)
N(1)–Mn(2)–N(3)	138.36(8)	O(5)–Mn(2)–N(2)	131.79(7)
N(2)–Mn(2)–N(3)	68.40(8)	O(5)–Mn(2)–N(3)	135.77(8)
O(5)–Mn(2)–N(2)	169.61(7)	O(5)–Mn(2)–O(4a)	112.52(7)
O(5)–Mn(2)–N(3)	120.93(7)	O(6)–Mn(2)–N(1)	84.12(8)
O(8)–Mn(2)–N(1)	98.90(8)	O(6)–Mn(2)–N(2)	87.61(7)
O(8)–Mn(2)–N(2)	101.42(8)	O(6)–Mn(2)–N(3)	93.98(8)
O(8)–Mn(2)–N(3)	87.02(7)	O(6)–Mn(2)–O(4a)	165.58(8)
		N(1)–Mn(2)–N(2)	66.73(7)
Mn(1)–O(5)–Mn(2)	112.83(8)	N(1)–Mn(2)–N(3)	135.77(8)
Mn(2)–N(1)–O(1)	125.2(2)	N(1)–Mn(2)–O(4a)	84.64(8)
Mn(2)–N(3)–O(2)	128.6(1)	N(2)–Mn(2)–N(3)	69.04(8)
O(3)–C(10)–O(4)	127.9(3)	N(2)–Mn(2)–O(4a)	96.20(8)
O(5)–C(11)–O(6)	127.6(3)	N(3)–Mn(2)–O(4a)	100.37(8)
O(7)–C(12)–O(8)	126.4(2)		
		Mn(1)–O(5)–Mn(2)	111.70(8)
		Mn(2)–N(1)–O(7)	127.1(1)
		Mn(2)–N(3)–O(8)	122.2(1)
		O(1)–C(1)–O(2)	125.4(2)
		O(3)–C(3)–O(4)	124.4(2)
		O(5)–C(5)–O(6)	119.8(2)

Acknowledgments

A. E. thanks the Ministerio de Ciencia y Tecnología (Spain), project CTQ2006-01759 for financial support of this research.

[1] C. J. Milios, T. C. Stamatatos, S. P. Perlepes, *Polyhedron* **2006**, *25*, 134–194.
[2] a) C. J. Milios, E. Kefallonti, C. P. Raptopoulou, A. Terzis, R. Vicente, N. Lalioti, A. Escuer, S. P. Perlepes, *Chem. Commun.* **2003**, 819–821; b) C. J. Milios, T. C. Stamatatos, P. Kyritsis, A. Terzis, C. P. Raptopoulou, R. Vicente, A. Escuer, S. P. Perlepes, *Eur. J. Inorg. Chem.* **2004**, 2885–2901.
[3] O. Roubeau, L. Lecren, Y. G. Li, X. F. Le Goff, R. Clerac, *Inorg. Chem. Commun.* **2005**, *8*, 314–318.
[4] C. Papatriantafyllopoulou, C. P. Raptopoulou, A. Escuer, C. J. Milios, *Inorg. Chim. Acta* **2007**, *360*, 61–68.
[5] C. Dendrinou-Samara, C. M. Zaleski, A. Evagorou, J. W. Kampf, V. L. Pecoraro, D. P. Kessissiglou, *Chem. Commun.* **2003**, 2668–2669.
[6] a) I. Vasilevsky, R. E. Stenpkamp, E. C. Lingafelter, N. J. Rose, *J. Coord. Chem.* **1988**, *19*, 171–187; b) B. C. Unni Nair, J. E. Sheats, R. Poteciello, D. Van Engen, V. Petrouleas, G. C. Dismukes, *Inorg. Chem.* **1989**, *28*, 1582–1587; c) R. E. Marsh, *Inorg. Chem.* **1990**, *29*, 572–573; d) C. W. Glynn, M. M. Turnbull, *Trans. Met. Chem.* **2002**, *27*, 822–831.
[7] a) S. Khanra, T. Weyhermüller, P. Chaudhuri, *Dalton Trans.* **2007**, 4675–4680; b) T. C. Stamatatos, B. S. Luisi, B. Moulton, G. Christou, *Inorg. Chem.* **2008**, *47*, 1134–1144.
[8] a) K. Hübner, H. W. Roesky, M. Noltemeyer, R. Bohra, *Chem. Ber.* **1991**, *124*, 515–517; b) K. Tsuneyoshi, H. Kobayashi, H. Miyamae, *Acta Crystallogr., Sect. C* **1993**, *49*, 233–236; c) D. Maspoch, J. Gómez-Segura, N. Domingo, D. Ruiz-Molina, K. Wurst, C. Rovira, J. Tejada, J. Veciana, *Inorg. Chem.* **2005**, *44*, 6936–6938; d) X. H. Bu, M. L. Tong, Y. B. Xie, J. R. Li, H. C. Chang, S. Kitagawa, J. Ribas, *Inorg. Chem.* **2005**, *44*, 9837–9846.
[9] a) E. V. Amel'chenkova, T. O. Denisova, S. E. Nefedoy, *Mendeleev Commun.* **2004**, *14*, 103–104; b) C. E. Anson, R. Langer, L. Ponikiewski, A. Rothenberger, *Inorg. Chim. Acta* **2005**, *358*, 3967–3973; c) B. Kang, M. Kim, J. Lee, Y. Do, S. Chang, *J. Org. Chem.* **2006**, *71*, 6721–6727.
[10] a) S. Menage, S. E. Vitols, P. Bergerat, E. Codjovi, O. Kahn, J. J. Girerd, M. Guillot, X. Solans, T. Calvet, *Inorg. Chem.* **1991**, *30*, 2666–2671; b) R. A. Reynolds III, W. R. Dunham, D. Coucouvanis, *Inorg. Chem.* **1998**, *37*, 1232–1241; c) B. H. Ye, X. M. Chen, F. Xue, L. N. Ji, T. C. W. Mak, *Inorg. Chim. Acta* **2000**, *299*, 1–8; d) G. Fernández, M. Corbella, J. Mahia, M. A. Maestro, *Eur. J. Inorg. Chem.* **2002**, 2502–2510; e) M. Kloskowski, D. Pursche, R. D. Hoffmann, R. Pöttgen, M. Läge, A. Hammerschmidt, T. Glaser, B. Krebs, *Z. Anorg. Allg. Chem.* **2007**, *633*, 106–112.
[11] a) M. Viertelhaus, H. Henke, C. E. Anson, A. K. Powell, *Eur. J. Inorg. Chem.* **2003**, 2283–2289; b) Z. Wang, B. Zhang, T. Otsuka, K. Inoue, H. Kobayashi, M. Kurmoo, *Dalton Trans.* **2004**, 2209–2216; c) X. Y. Wang, H. Y. Wei, Z. M. Wang, Z. D. Chen, S. Gao, *Inorg. Chem.* **2005**, *44*, 572–583; d) Z. Wang, B. Zhang, K. Inoue, H. Fujiwara, T. Otsuka, H. Kobayashi, M. Kurmoo, *Inorg. Chem.* **2007**, *46*, 437–445.
[12] G. M. Sheldrick, *SHELXS*, *A Computer Program for Determination of Crystal Structures*, University of Göttingen, Germany, **1997**.
[13] G. M. Sheldrick, *SHELX97*, *A Computer Program for Determination of Crystal Structures*, University of Göttingen, Germany, **1997**.
[14] *International Tables of X-ray Crystallography*, Kynoch Press, Birmingham, UK, **1974**, vol. IV, pp. 99–100, 149.

Received: May 30, 2008
Published Online: October 10, 2008

